

Geometric structure of $p(2 \times 2)$ -S/Cu(001) determined by medium-energy ion scattering

Q. T. Jiang, P. Fenter, and T. Gustafsson

*Department of Physics and Astronomy, and Laboratory for Surface Modification, P.O. Box 849,
Rutgers—The State University of New Jersey, Piscataway, New Jersey 08855-0849*

(Received 7 May 1990)

We have determined the geometric structure of the $p(2 \times 2)$ -S/Cu(001) surface with medium-energy ion scattering. There are qualitative features in our data that clearly show that sulfur adsorption does *not* induce large atomic rearrangements of the Cu substrate. A detailed analysis based on Monte Carlo simulations shows that the sulfur atoms are located 1.30 Å above the copper surface. The first Cu layer moves outwards by 0.02 Å, and the top-layer Cu atoms move laterally away from the adsorbate by 0.03 Å. This results in a S—Cu bond length of 2.25 Å. Our results are compared with earlier contradictory results on this controversial system. We find excellent agreement with a recent low-energy electron diffraction study.

I. INTRODUCTION

By adsorbing approximately a $\frac{1}{4}$ monolayer of sulfur on Cu(001), a clear and sharp $p(2 \times 2)$ low-energy electron diffraction (LEED) pattern can be produced. Detailed structural work on this system includes quantitative LEED studies,^{1,2} analysis of angle-resolved-photoemission extended fine-structure (ARPEFS),³⁻⁵ and a study utilizing a combination of x-ray standing wave (XSW) and surface-extended x-ray-adsorption fine structure (SEXAFS).⁶ There is general agreement that the S atoms chemisorb above the four-fold hollow sites of the Cu(001) surface, and that the S—Cu bond length is ~ 2.26 Å. However, beyond this there is considerable controversy. Detailed results have been given based on LEED (Ref. 2) and ARPEFS.⁴ Both models invoke adsorbate-induced substrate reconstructions. However, these two models differ as to the magnitude, and more surprisingly, the signs of these rearrangements. In the LEED model, the first-layer Cu atoms move horizontally *away* from the sulfur atom (we will refer to this as *positive pairing*). There is also a small expansion of the vertical separation d_{12} between the first two layers ($\Delta d_{12} = +1\%$, where $\Delta d_{12} = 0\%$ corresponds to a bulklike value). In the ARPEFS model, the pairing is in the opposite sense in that the first-layer Cu atoms move horizontally *toward* the sulfur atom (*negative pairing*), and there is a large contraction of the first interplanar separation ($\Delta d_{12} = -8\%$) as well as a substantial buckling in the second layer.

The structure of the clean Cu(001) surface is simple and well characterized. All studies agree that this surface exhibits an oscillatory relaxation of the first few interlayer spacings,⁷⁻¹⁰ as observed for many metal surfaces. The magnitude of the effect is small, as the fcc(001) surface is close-packed. Very recently, we have found that

$$\Delta d_{12} = -2.4\%, \text{ while } \Delta d_{23} = +1\%.^{11}$$

Below, we present the results from a study using medium-energy ion scattering (MEIS) with channeling and blocking of the structure of the $p(2 \times 2)$ -S/Cu(001) system. MEIS is a quantitative and intuitive surface structure tool. As we will demonstrate, there are straightforward features in our spectra that demonstrate that large-scale substrate reconstructions do not occur. We arrive at a structural model that is in remarkably good agreement with the LEED model, but in severe disagreement with the model based on ARPEFS.

The outline of this paper is as follows: In Sec. II, the experimental procedures are described. In Sec. III, the procedure used in the detailed data analysis for extraction of surface-structural parameters is presented. In Sec. IV, our results are compared with earlier experimental work. Finally, some conclusions are drawn in Sec. V.

II. EXPERIMENT

Medium-energy ion scattering is a surface structural technique that utilizes a 30–400 keV beam of light ions (in our case protons) incident in a high-symmetry crystallographic direction on a crystal (*channeling*).^{12,13} In a rigid, bulk-terminated lattice, only the first atom along each row of atoms in the target is visible to the incident beam. The rest of the atoms in the row are said to be shadowed by the first atom. In any real crystal, thermal vibrations and/or distortions of the atomic positions at the surface will cause subsurface atoms to have nonzero hitting probabilities. For common experimental parameters, the hitting probabilities along the row fall off rapidly to zero.

In MEIS the angular distribution of the backscattered ions is measured over a wide angular range. Ions scattered from deeper layers will exit the crystal freely, except along those directions where they are blocked by

other atoms above them in the surface region. This will result in a lower yield (a blocking dip) in those directions. If the surface atoms sit in bulk lattice sites, these blocking dips should be observed exactly in the bulk crystallographic directions. If the top interlayer spacing is contracted, the surface blocking directions will shift to smaller scattering angles, while the inverse would be true for an expansion. By observing such differences, one can get a direct understanding of the main features of the surface structure.

To extract detailed structural parameters, one uses the fact that the ion-surface interaction law is known in detail¹⁴⁻¹⁶ in the energy range we work in (a weakly screened Coulomb potential is appropriate). One then performs a Monte Carlo simulation of the experiment for a trial surface structure and compares this with the experimental data. By varying this trial structure and performing a *R*-factor analysis, the optimal structural parameters can be determined. As the scattering cross section is known,^{17,18} the experimental data can be measured in absolute units; that is the data can be directly converted to the number of atoms visible to the ion beam per (1×1) unit cell. All input parameters are therefore physically meaningful and no arbitrary fitting parameters are involved. A basic strength of MEIS is that one has a good sense for the structural parameters based upon just a simple inspection of the data. The actual functional choice of *R* factor is not particularly crucial due to the fact that MEIS is a quantitative technique and both calculation and experiment are done in absolute units.

The largest uncertainty in the interpretation of the experimental data is associated with the modeling of the surface vibrational amplitudes (in our case both for the copper atoms and the adsorbate), which are not known *a priori*. Ion scattering gives consistent evidence for enhancements of the vibrational amplitudes in the surface region. We use isotropic vibrational amplitudes and let the enhancement decay into the bulk by a factor of 2 between adjacent layers. The results presented below are not sensitive to the exact way this decay is modeled.¹⁹ Another important effect is the correlation of the vibrational motion of adjacent atoms.^{20,21} Since ion-scattering experiments are only sensitive to the relative atomic motions, vibrational correlations for adjacent atoms should be taken into account. We use an effective vibrational amplitude *U'* which is obtained by rescaling the one-dimensional vibrational amplitude *U*: $U' = U \sqrt{1-C}$. Here, *C* is the correlation coefficient of atoms *i* and *j*, defined as $C_{ij} = (\langle U_i U_j \rangle) / \langle U_i^2 \rangle$, where the denominator is the mean square of atomic displacement and $\langle \rangle$ denotes a thermal averaging. *C_{ij}* depends upon the distance between atoms *i* and *j*, and both *U* and *C_{ij}* are calculated in the Debye model. A single correlation coefficient *C* is applied to all ion paths with the same incident direction. This procedure has been used successfully earlier in analysis of other ion-scattering data.²²⁻²⁴ *C* is calculated to be 0.37 and 0.17 for ions incident along the [10 $\bar{1}$] direction (45° off normal) and along the [30 $\bar{1}$] direction (71.56° off normal), respectively, in the (010) zone and 0.19 for the [1 $\bar{1}$ $\bar{2}$] direction (35.26° off normal) in the (110) zone. The bulk Debye temperature of Cu is

320 K, and the bulk thermal vibrational amplitude at room temperature is 0.0829 Å.²³

A clean Cu(001) surface was prepared by standard sputtering and annealing cycles until a sharp (1×1) LEED pattern appeared. The cleanliness was monitored by Auger-electron spectroscopy (AES) using a double-pass cylindrical mirror analyzer. This surface was then exposed to 22 L [1 L (langmuir) = 10⁻⁶ Torr s] H₂S. At this point, weak and broad half-order LEED spots were observed. By annealing the sample to 300°C for a few minutes a sharp *p*(2×2) LEED pattern was obtained. The sample was checked with AES occasionally in the course of the ion-scattering experiments, showing no detectable impurities. The base pressure in the ultrahigh-vacuum (UHV) system was ~10⁻¹⁰ torr. The measurements were carried out with a beam energy of 100 keV at room temperature.

The scattered ions were measured with a high-resolution electrostatic toroidal energy analyzer with an angular acceptance of 24° and an angular resolution of ~0.3°. The analyzer is rotatable to permit a selection of geometries in the scattering plane. Since the analyzer measures charged particles only, neutralization effects have to be corrected for. The ratio of the charged particle flux to the total number of exiting particles (*P*⁺) was measured with a solid-state detector equipped with electrostatic deflection plates for the energy range 80 to 200 keV. *P*⁺ was found to be a slowly varying function of energy, equal to 0.77 at 100 keV, and is known to be independent of exit angle.²⁵ Adsorption of a ¼ overlayer of sulfur did not alter the fraction of the charged particles, which is consistent with measurements of other chemisorption systems.²⁵

A typical energy distribution curve is shown in Fig. 1. The leading peak is due to those protons that have scattered off Cu surface atoms. At lower energies, a weaker peak is observed due to ions scattered off sulfur atoms. The energy of this peak is lower, as the mass of the adsor-

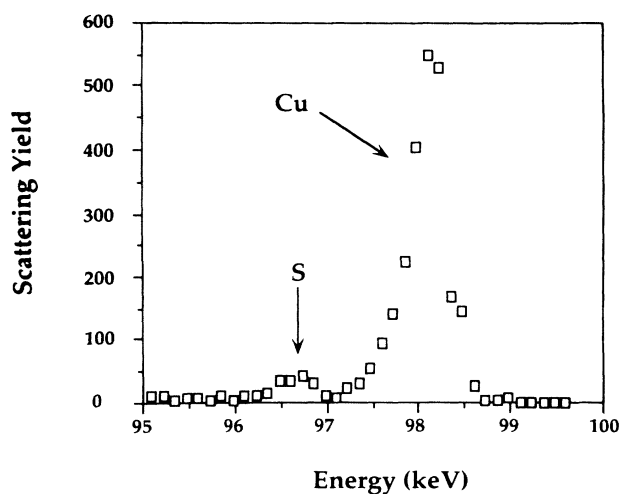


FIG. 1. Energy spectrum of backscattered protons from the *p*(2×2)-S/Cu(001) surface for a 100 keV beam incident along the [30 $\bar{1}$] direction, detected in the (010) scattering plane around a scattering angle $\theta_s = 64^\circ$. Note that the Cu and S signals are clearly resolved.

bate is smaller. The relative size of the peaks is due to the difference in scattering cross sections of the two atoms, which depend on the square of their nuclear charges, and to the number of atoms seen by the beam per (1×1) unit cell. The two peaks are well resolved so that we can measure the S and Cu scattering yields independently. From these data, the sulfur coverage was determined to be 0.23 ± 0.05 monolayers. Unless otherwise noted, all yields in this paper refer to Cu yields. The spectra were inspected carefully for evidence of beam damage. No effect was found even with a beam dose 1 order of magnitude higher than we used in the experiment.

III. DATA ANALYSIS

Figure 2(a) is a schematic top view of a $p(2 \times 2)$ overlayer of S on Cu(001). The surface has fourfold symmetry, and the S atoms are known to sit in fourfold hollow sites. ¹⁻⁶ There exist three inequivalent second-layer Cu sites, labeled C, O, and A. The C site is immediately underneath the adsorbate, while there is no adsorbate directly above the A and O sites. Therefore, the magnitude of the vertical relaxation of the Cu atoms in these three sites may be different. Figure 2(b) shows a side view in the (010) zone with the O site projected in the plane. MEIS measurements were carried out in two scattering zones: (010) and (110). The incident directions we used were the $[10\bar{1}]$ and $[30\bar{1}]$ in (010) zone, and the $[\bar{1}\bar{1}\bar{2}]$ in (110) zone.

In the following, we present our data analysis for (010) zone scattering with $[10\bar{1}]$ incident direction (Fig. 3). In this scattering geometry, only the first-layer Cu atoms are completely visible to the incident beam, i.e., these atoms have a hitting probability equal to 1. The calculated hitting probability (for 100 keV protons) decreases to 0.71 for the second layer, 0.26 for the third layer, 0.05 for the fourth layer, and less than 0.03 for the deeper layers. The backscattered ions are detected in an angular range of 50° , which includes the $[101]$, $[301]$, and $[501]$ crystallographic directions. The Cu yield for the adsorbate covered surface is compared with that from the clean surface [Fig. 3(b)]. The two sets of data are quite similar over the whole angular range. This suggests that the surface structure of the substrate is close to that of the clean Cu(001) structure. As the surface relaxations of Cu(001) are small, ⁷⁻¹¹ the atomic displacements on the adsorbate covered surface should then also be small.

The two spectra in Fig. 3(b) are similar, but not identical. For instance, around 64° scattering angle, the two blocking dips do not line up exactly. A more detailed view of these data are shown in Fig. 3(c). One can see that the whole S/Cu spectrum has been shifted slightly towards larger angles. This shows that with respect to clean Cu(001), there is a slight expansion. This would bring the Cu surface back towards bulklike sites. An exception to this shift is seen on the left-hand side of the $[101]$ blocking dip in Fig. 3(b) (90° scattering angle). This behavior is due to blocking of sulfur atoms and will be discussed later.

The differences between the two proposed models described in Sec. I is most clearly observable around the

$[101]$ direction (90° scattering angle). We show simulations based on the two proposed models in this geometry in Fig. 4. Since d_{12} is strongly contracted in the ARPEFS model, there is a large shift of the surface blocking dip towards smaller scattering angles for this model. As the atomic rearrangements in the LEED model are small, no significant shift occurs in this model. Our data are in quite good agreement with the LEED model and disagree with ARPEFS.

We have searched for the optimal structural parameters with a *R*-factor analysis. ²⁴ The *R* factor is a measure

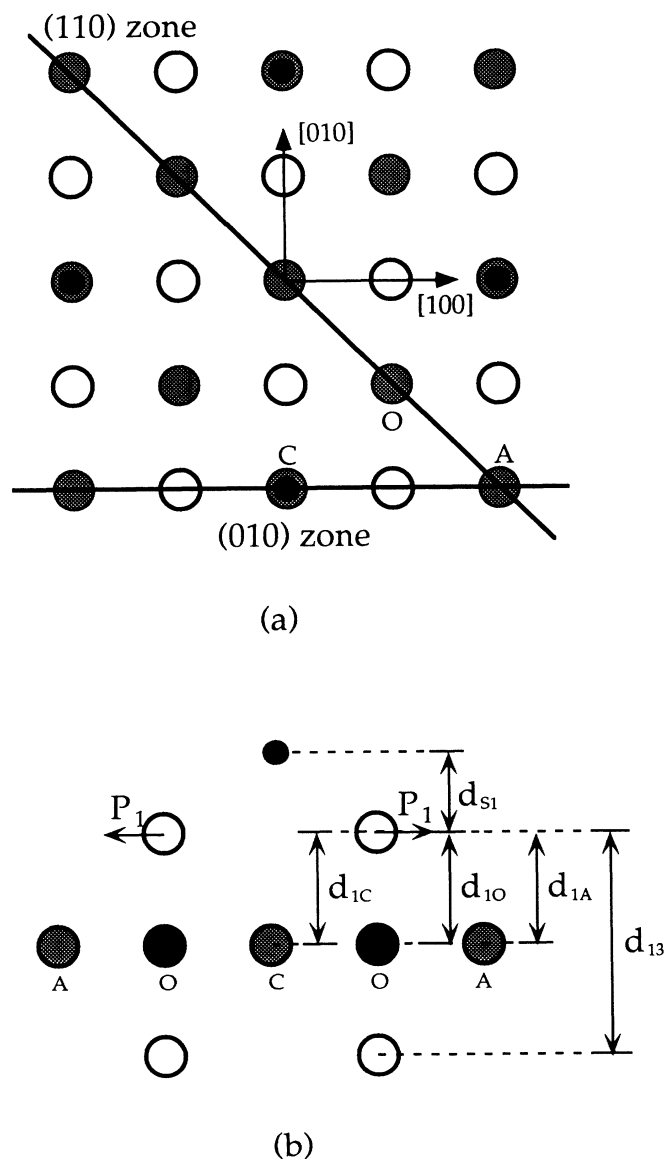


FIG. 2. (a) Top view of the $p(2 \times 2)$ -S/Cu(001) surface. Open (shaded) circles are the first- (second-) layer Cu atoms. Sulfur atoms (solid circles) sit in fourfold hollow sites above the second-layer Cu atoms. The three inequivalent Cu sites in the second layer are labeled C, O, and A. Solid lines indicate the two scattering planes used in this study. (b) Side view of the crystal along the (010) plane. The O site in the second layer has been projected onto this plane.

of the fit between simulation and experiment with lower R values signifying better agreement with experiment. In this way, atomic positions can be determined with an accuracy of a few hundredths of an angstrom. Because of the low coverage and low atomic number for S, the MEIS angular spectrum does not show large blocking effects due to the S atoms. Therefore the Cu parameters are easier to determine than the S parameters. We show in Fig. 5 a set of R -factor contours for variations of the two most sensitive Cu parameters: The first-to-third layer spacing d_{13} and the surface vibrational amplitude (expressed as its ratio to the bulk value U_s/U_b). There is a clear minimum for $d_{13} = 3.63 \pm 0.03$ Å, and $U_s/U_b = 1.83$. The bulk double layer spacing is 3.61 Å,

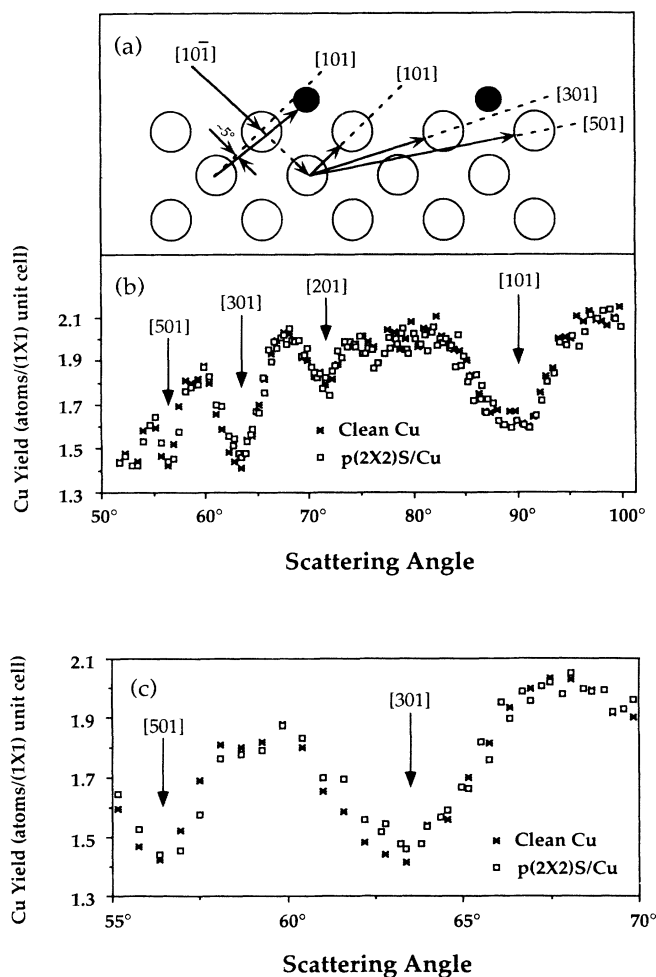


FIG. 3. (a) Scattering geometry for protons incident along the $[10\bar{1}]$ direction and detected in an angular range including the $[101]$, $[301]$, and $[501]$ directions in the (010) plane. There are two different and independent (010) scattering planes, but only one is shown. (b) The experimental backscattered yield from S/Cu (open squares) and clean Cu (asterisks) as a function of scattering angle for 100 keV protons. The crystallographic direction associated with each blocking dip is indicated. (c) An enlarged version of (b) around 64° scattering angle.

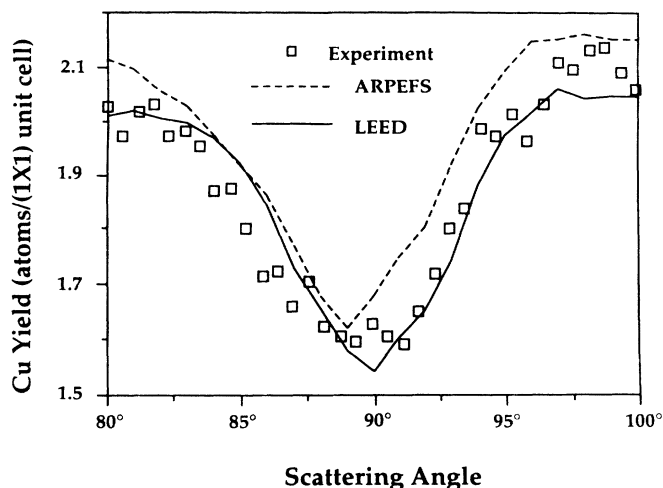


FIG. 4. Experimental yield and simulations of the LEED (Ref. 2) (solid line) and ARPEFS (Ref. 4) (dashed line) models near the $[101]$ blocking direction (90°). The MEIS data, which are in good agreement with the LEED model, are indicated by open squares.

so we find a slight expansion of the spacing between the first and third layer of 0.02 Å. As $U_s = 1.83U_b = 0.15$ Å, the surface vibrational amplitude has been enhanced by 83%, which corresponds a surface Debye temperature $\Theta_s = 175$ K.

The $p(2 \times 2)$ symmetry allows for a buckling of the second Cu layer, corresponding to different spacings d_{1C} , d_{10} and d_{1A} . These three parameters all have a strong effect upon the scattered yield. Therefore all three parameters need to be varied simultaneously in the simulation. The R -factor contours for varying d_{10} and d_{1A} are shown in Fig. 6(a), while in Fig. 6(b) d_{1C} and d_{1A} are varied. Each of the contours has a clear and well-defined minimum and the d_{1A} values in the two contours are the

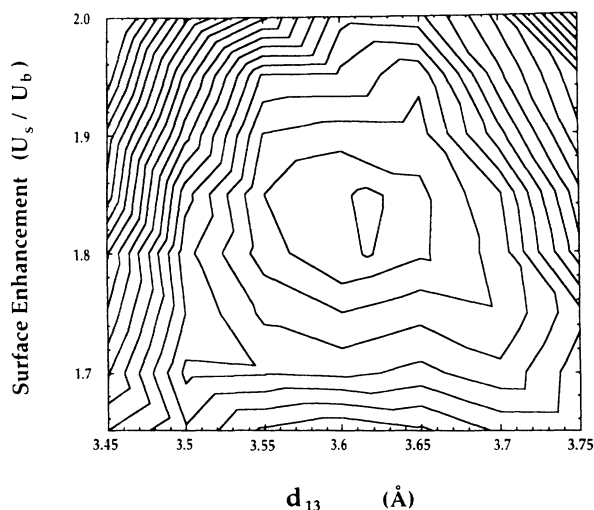


FIG. 5. R -factor contour map for the S/Cu data in Fig. 3(b) as a function of the first-to-third layer spacing d_{13} and the surface vibrational enhancement U_s/U_b .

same. All the three spacings are equal to 1.81 Å, which is within 0.02 Å of the bulk value. Consequently, although a buckling is allowed by symmetry, we find no evidence for such an effect.

Compared with Cu, the S related parameters affect the angular spectrum in a less direct way. We therefore assessed all the Cu parameters (except the pairing in the first layer) as accurately as possible before varying the S parameters. Figures 7(a) and 7(b) show the R -factor curves versus the height of the sulfur atom over the first Cu layer (d_{S1}), and the sulfur vibrational amplitude U_s , respectively. In Fig. 7(a) a distinct minimum is found, $d_{S1} = 1.30$ Å. We estimate the error in this coordinate to be ± 0.05 Å. The R -factor curve for the sulfur vibrational amplitude [Fig. 7(b)] is quite asymmetric with a minimum around 0.23 Å.

Finally we searched for a lateral movement (pairing) of the first-layer Cu atoms. We varied this parameter last since previous studies^{2,4} show that the pairing, if present, is a very small effect. Also for the scattering geometries we used, we are less sensitive to horizontal displacements. Figure 8 shows the R -factor curve as a function of pair-

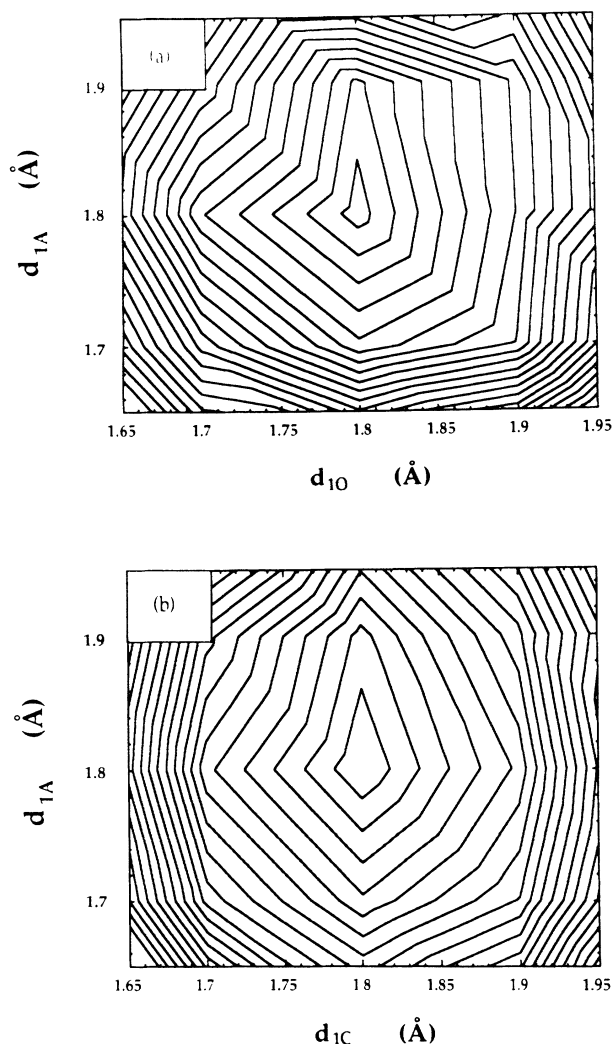


FIG. 6. R -factor contour maps for the S/Cu data in Fig. 3(b) as a function of (a) d_{10} and d_{1A} , and (b) d_{1C} and d_{1A} .

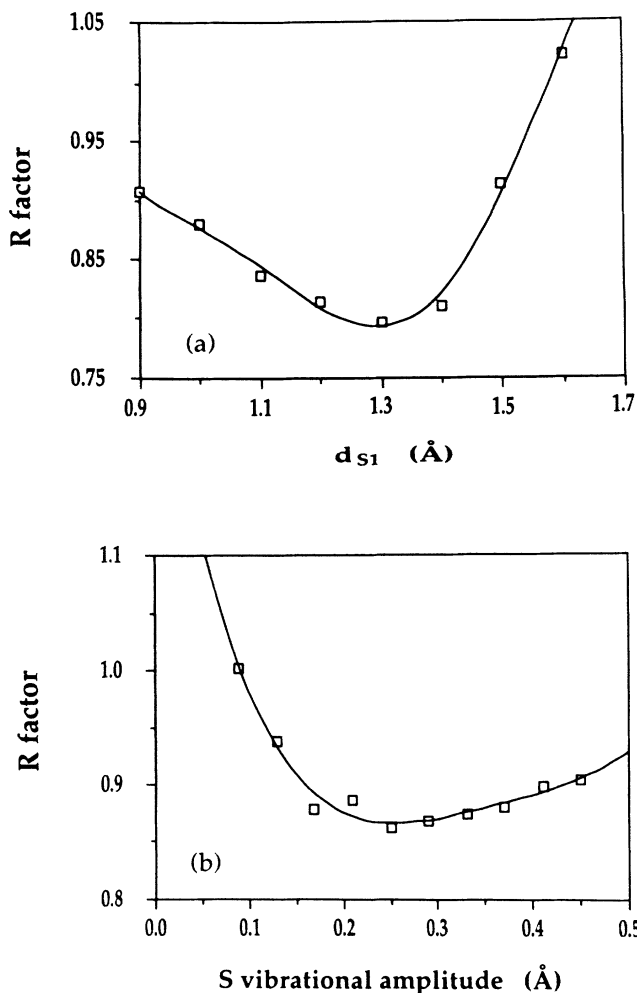


FIG. 7. R factor as a function of (a) sulfur to copper vertical distance d_{S1} , (b) sulfur vibrational amplitude for the S/Cu data in Fig. 3(b). Note that the R factors have been multiplied with a factor of 10^2 .

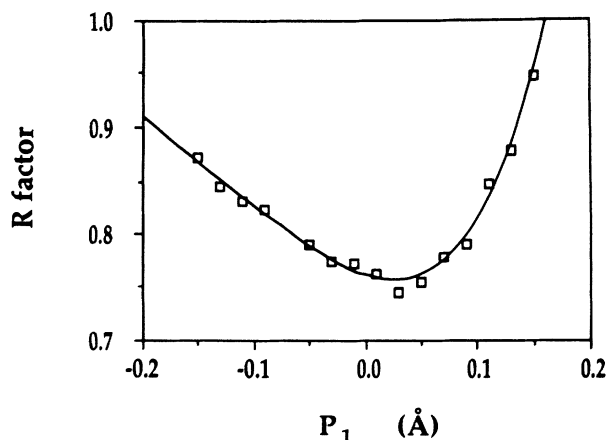


FIG. 8. R factor as a function of the horizontal movement of the first-layer Cu atoms (pairing) for the S/Cu data in Fig. 3(b). Note that the R factor has been multiplied with a factor of 10^2 .

ing. A minimum is clearly observed at $+0.03 \text{ \AA}$. We estimate the error on this determination to be $\pm 0.03 \text{ \AA}$.

In the above, we described the procedure for the initial search for the structural and vibrational parameters. To take into account interdependence of parameters, we repeated the whole process until no significant changes of all simulated parameters resulted. The values quoted above are our best fit values.

The data for 71.6° incidence in the (010) zone and 35.3° incidence in the (110) zone were also analyzed through the procedure mentioned above. Unlike the (010) zone scattering, where only the first-layer Cu atoms are completely visible to the incident beam for both 45.0° and 71.6° incidence, the first two layers of Cu atoms are completely visible to the incident beam for the (110) zone scattering. Therefore the yield for the (110) zone scattering is much larger than that of the (010) zone scattering, while the sulfur scattering in both zones remains roughly the same. In all three geometries, the data converged to the same model within the error bars mentioned above, ensuring that the minimum we found is a global minimum.

All structural parameters have now been determined. Figures 9(a) and 9(b) show a detailed comparison between our data in two scattering geometries and a Monte Carlo simulation for our optimal structure. Although minor differences exist in the depth of the blocking dips, which could be due to small remaining uncertainties like surface defects, the simulations agree very well with the experiment. The vibrational amplitudes we obtain in each of the scattering geometries are the same. As different scattering geometries weight the in-plane and out-of-plane vibrational amplitudes differently, this implies that there is no significant anisotropy of the vibrational amplitudes.

We would now like to address the lack of the shift of the $[10\bar{1}]$ blocking dip in (010) zone [Fig. 3(b)]. Based on our model and the scattering geometry displayed in Fig. 3(a), simple trigonometric arguments show that the blocking of the flux from the second-layer Cu atoms due to the sulfur atoms will occur at an angle of $\sim 85^\circ$. It will therefore overlap the Cu—Cu blocking dip around 90° . Since the sulfur coverage is small (0.25 ML) and the sulfur vibrational amplitude is large (0.23 \AA), the sulfur blocking is expected to be very shallow, resulting in a

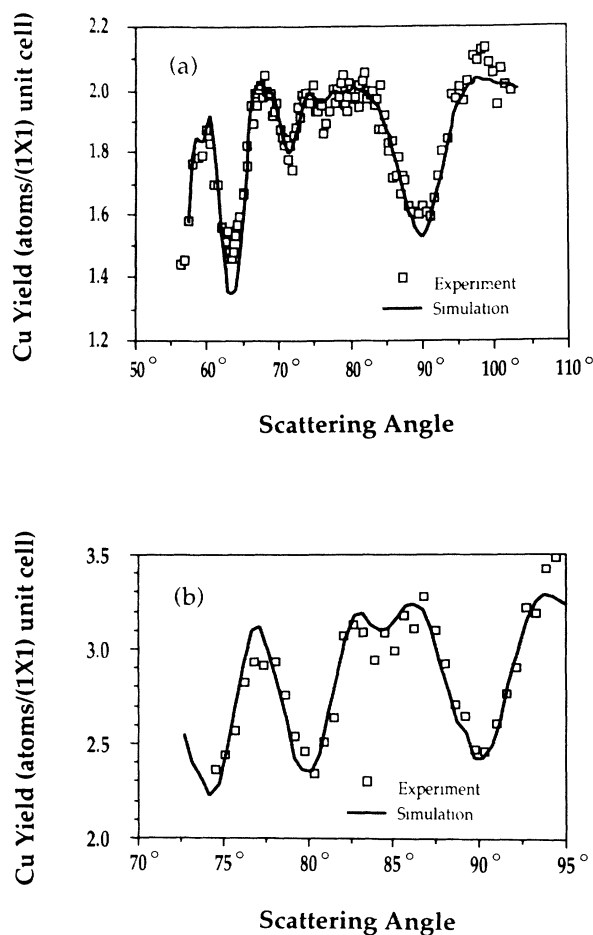


FIG. 9. Experimental data (open squares) and simulations for our best structure (solid lines) shown in (a) for protons incident along the $[10\bar{1}]$ direction in the (010) plane, and in (b) for protons incident along the $[1\bar{1}\bar{2}]$ direction in the (110) plane.

slight asymmetry of the Cu blocking dip. This is the cause of the unexpected behavior (no shift towards larger angles) at the low-angle side in the blocking dip around 90° in Fig. 3(b), referred to above. The flux from the first- and second-layer Cu atoms will also be blocked by sulfur atoms, which results in a lowering in S/Cu yield around 80° scattering angle. This is why the S/Cu yield is statist-

TABLE I. Structural parameters for $p(2\times 2)$ -S/Cu(001) determined by different techniques. The bulk interplanar separations d_{12} and d_{13} are equal to 1.81 and 3.61 \AA , respectively.

	MEIS ^a	LEED (Ref. 2)	ARPEFS (Ref. 4)	XSW SEXAFS (Ref. 6)	X-ray scattering (Ref. 27)	Clean Cu(001) (Ref. 11)
d_{S1}	1.30	1.29	1.42	1.44 ^b	1.19	
d_{1C}	1.81	1.84	1.62			1.77
d_{1O}	1.81	1.83	1.65			1.77
d_{1A}	1.81	1.81	1.74			1.77
d_{13}	3.63	3.65	3.55			3.58
S—Cu	2.25	2.26	2.26	2.31	2.19	
P_1	+0.03	+0.04	-0.05		+0.03	0

^aResults of the present study.

^bCalculated in Ref. 6 assuming no substrate reconstruction.

ically lower than that of clean surface around 80° [Fig. 3(b)].

IV. DISCUSSION

Our MEIS results show clear and direct evidence that adsorption of a $p(2 \times 2)$ overlayer of S on Cu(001) does not induce a large substrate relaxation. The atomic rearrangements in the substrate are even smaller than for the clean Cu(001) surface, and are only slightly different from an ideally bulk-terminated structure.

The structural parameters determined by different techniques are given in Table I. Although the results for the sulfur position (d_{S1}) are very different for different techniques, there is wide agreement on a S—Cu bond length of $\approx 2.25 \text{ \AA}$. This effect results in large differences in the measured values of the first layer pairing (P_1), which is directly related to d_{S1} for a given value of the bond length. Our values of d_{S1} (1.30 \AA) and P_1 (+0.03 \AA) are in very good agreement with the LEED model and also with an inelastic electron scattering measurement, which yielded $d_{S1} = 1.30 \pm 0.05 \text{ \AA}$.²⁶ Very recently, x-ray diffraction experiments, which are very sensitive to lateral distortions, found that P_1 is equal to +0.03 \AA ,²⁷ again in excellent agreement with our results. Relative to the ARPEFS model, the sulfur atoms in the LEED and MEIS models are located closer to the topmost Cu layer. Therefore, with a fixed S—Cu bond length, the nearest Cu atoms in the LEED and MEIS models are pushed away laterally, and the opposite is found in the ARPEFS model.

We find the first Cu interlayer spacing (d_{12}) to be essentially equal to the bulk value, in contrast to the large contraction found for the ARPEFS model ($\sim 8\%$), but in good agreement with the LEED model. Although both LEED and ARPEFS found a buckling in the second layer, we do not find any evidence for this effect. The buckling in the LEED model is quite small though, and the three values of d_{12} only vary by 0.03 \AA , which is within the error bars of both MEIS and LEED. Again, the ARPEFS result is very different, claiming a buckling amplitude of 0.12 \AA . With respect to d_{13} , there are also differences between MEIS and LEED on the one hand ($\Delta d_{13} = +0.02$ and $+0.04 \text{ \AA}$, respectively) and ARPEFS on the other ($\Delta d_{13} = -0.06 \text{ \AA}$).

It is interesting to relate our model to our recent results for the clean Cu(001) surface ($\Delta d_{12} = -2.4\%$ and $\Delta d_{23} = +1\%$).¹¹ The effect of the sulfur adsorption is to bring the outermost layer back to a bulk terminated location and to cause a gentle lateral outward movement of

the Cu atoms closest to the adsorbate. The second-layer Cu atoms are not affected appreciably by sulfur adsorption, probably because the separation between the S atoms and the second-layer Cu atoms is too large. With respect to clean Cu(001), significant changes in the S/Cu substrate occur only in the first layer. For both systems, the surface vibrational amplitudes have been found to be greatly enhanced. We have looked for vibrational anisotropy in the S/Cu system, but the vibrations are well described as isotropic.

The outward movement of the first Cu layer induced by S adsorption can be understood through a simple picture. The common trend of relaxations at clean metal surfaces has been explained successfully by Finnis and Heine²⁸ with an ion-lattice model, in which the electron surface tension causes the electrons to smooth out the surface corrugation. This electron redistribution induces an effective electrostatic force on the surface resulting in a surface contraction. Upon adding a $\frac{1}{4}$ monolayer of S on Cu(001), the charge transfer between S and Cu will again result in a charge redistribution in the surface region. Since the electronegativity of S is greater than that of Cu, the Cu electrons will move outwards towards the S atoms, removing the electrostatic driving force for an inwards relaxation. This kind of phenomenon has been observed in similar chemisorption systems like S/Ni(110) (Ref. 29) and O/Ni(001).^{25,30}

V. CONCLUSIONS

We have investigated the surface structure of the $p(2 \times 2)$ -S/Cu(001) system with MEIS. The data show clear and direct evidence that the adsorbate does not induce a large reconstruction of the substrate. The effect of the sulfur adsorption is to move the outermost layer of Cu atoms outward and to make the Cu atoms closest to the adsorbate move laterally away from the adatom. We have not detected any effects upon deeper layers. The structural parameters we obtain are very close to those found by LEED, but disagree with ARPEFS results.

ACKNOWLEDGMENTS

We would like to thank Dr. F. Jona for stimulating our interest in this problem, Dr. R. Bartynski for lending us the Cu(001) crystal, and Mr. M. Chester, Mr. P. Statiris, and Mr. J. B. Zhou for their help. This research was supported by the National Science Foundation (NSF) Grant No. DMR-8703897.

¹H. C. Zeng, R. N. S. Sodhi, and K. A. R. Mitchell, Surf. Sci. **177**, 329 (1986).

²H. C. Zeng, R. A. McFarlane, and K. A. R. Mitchell, Phys. Rev. B **39**, 8000 (1989).

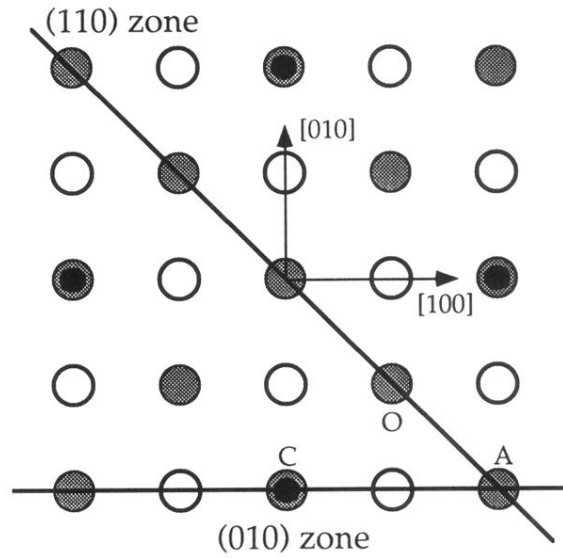
³J. J. Barton, C. C. Bahr, Z. Hussain, S. W. Robey, J. G. Tobin, L. E. Klebanoff, and D. A. Shirley, Phys. Rev. Lett. **51**, 272 (1983).

⁴C. C. Bahr, J. J. Barton, Z. Hussain, S. W. Robey, J. G. Tobin, and D. A. Shirley, Phys. Rev. B **35**, 3773 (1987).

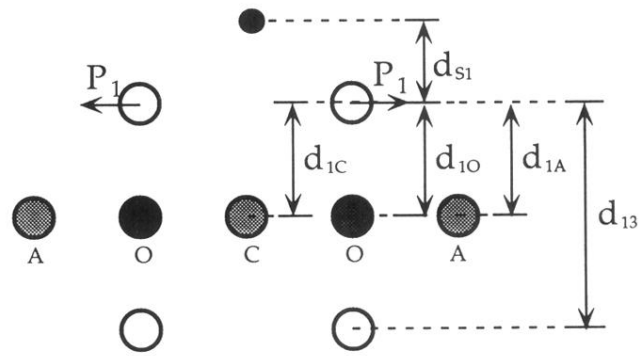
⁵D. A. Shirley, L. J. Terminello, and C. C. Bahr, Phys. Rev. B **39**, 8003 (1989).

⁶J. R. Patel, D. W. Berreman, F. Sette, P. H. Citrin, J. E. Rowe, P. L. Cowan, T. Jach, and B. Karlin, Phys. Rev. B **40**, 1330 (1989).

- ⁷J. R. Noonan and H. L. Davis, *J. Vac. Sci. Technol.* **17**, 194 (1980).
- ⁸H. L. Davis and J. R. Noonan, *J. Vac. Sci. Technol.* **20**, 842 (1982).
- ⁹P. F. A. Alkemade, W. C. Turkenburg, and W. F. van der Weg, *Nucl. Instrum. Methods B* **15**, 126 (1986).
- ¹⁰D. M. Lind, F. B. Dunning, G. K. Walters, and H. L. Davis, *Phys. Rev. B* **35**, 9037 (1987).
- ¹¹Q. T. Jiang, P. Fenter, and T. Gustafsson (unpublished).
- ¹²J. F. van der Veen, *Surf. Sci. Rep.* **5**, 199 (1985).
- ¹³W. R. Graham, S. M. Yalisove, E. D. Adams, T. Gustafsson, M. Copel, and E. Törnqvist, *Nucl. Instrum. Methods B* **16**, 3831 (1986).
- ¹⁴G. Molière, *Z. Naturforsch. Teil 2A*, 133 (1947).
- ¹⁵J. P. Biersack and J. F. Ziegler, *Nucl. Instrum. Methods* **194**, 93 (1982).
- ¹⁶D. J. O'Connor and J. P. Biersack, *Nucl. Instrum. Methods B* **15**, 14 (1986).
- ¹⁷H. H. Andersen, F. Besenbacher, P. Loftager, and W. Möller, *Phys. Rev. A* **21**, 1891 (1980).
- ¹⁸A. Weber, H. Dahlmann, H. Mommsen, and W. Sarter, *Nucl. Instrum. Methods* **200**, 567 (1982).
- ¹⁹J. W. M. Frenken, R. G. Smeenk, and J. F. van der Veen, *Surf. Sci.* **135**, 147 (1983).
- ²⁰D. P. Jackson, B. M. Powell, and G. Dolling, *Phys. Lett.* **51A**, 87 (1975).
- ²¹D. P. Jackson and J. H. Barrett, *Comp. Phys. Commun.* **13**, 157 (1977).
- ²²J. W. M. Frenken, J. F. van der Veen, R. N. Barnett, U. Landman, and C. L. Cleveland, *Surf. Sci.* **172**, 319 (1986).
- ²³M. Copel, T. Gustafsson, W. R. Graham, and S. M. Yalisove, *Phys. Rev. B* **33**, 8110 (1986).
- ²⁴P. Fenter and T. Gustafsson, *Phys. Rev. B* **38**, 10 197 (1988).
- ²⁵J. W. M. Frenken, R. G. Smeenk, and J. F. van der Veen, *Surf. Sci.* **135**, 147 (1983).
- ²⁶Z. Q. Wu, M. L. Xu, Y. Chen, S. Y. Tong, M. H. Mohamed, and L. L. Kesmodel, *Phys. Rev. B* **36**, 9329 (1987).
- ²⁷E. Vlieg, I. K. Robinson, and R. McGrath, *Phys. Rev. B* **41**, 7896 (1990).
- ²⁸M. W. Finnis and V. Heine, *J. Phys. F* **4**, L37 (1974).
- ²⁹J. F. van der Veen, R. M. Tromp, R. G. Smeenk, and F. W. Saris, *Surf. Sci.* **82**, 468 (1979).
- ³⁰J. W. M. Frenken, J. F. van der Veen, and G. Allan, *Phys. Rev. Lett.* **51**, 1876 (1983).



(a)



(b)

FIG. 2. (a) Top view of the $p(2 \times 2)$ -S/Cu(001) surface. Open (shaded) circles are the first- (second-) layer Cu atoms. Sulfur atoms (solid circles) sit in fourfold hollow sites above the second-layer Cu atoms. The three inequivalent Cu sites in the second layer are labeled C, O, and A. Solid lines indicate the two scattering planes used in this study. (b) Side view of the crystal along the (010) plane. The O site in the second layer has been projected onto this plane.